Article ID: 1000-324X(2018)07-0798-07 **DOI:** 10.15541/jim20170387

Preparation of $Ce_xZr_{1-x}O_2$ with Combined Composition for Improved Pd-only Three-way Catalyst

LI Hong-Mei[1], LAN Li[1], CHEN Shan-Hu[2], LIU Da-Yu[1], WANG Wei[1], CHEN Yao-Qiang[3]

(1. College of Pharmacy and Biological Engineering, Chengdu University, Chengdu 610106, China; 2. Sinocat Environmental Technology Co., Ltd., Chengdu 611731, China; 3. Key Laboratory of Green Chemistry & Technology, Ministry of Education, College of Chemistry, Sichuan University, Chengdu 610064, China)

Abstract: Two special CeO_2-ZrO_2 composites with combined compositions were prepared by a simple sequential precipitation method. The effect of the combination styles on properties of the supported Pd-only three-way catalysts was investigated by means of X-ray diffraction (XRD), Raman spectroscopy, X-ray photoelectron spectroscopy (XPS), nitrogen adsorption/desorption, H_2-temperature programmed reduction (H_2-TPR), and oxygen storage capacity measurement (OSC). The results reveal that the structural and textural properties are modified for the two catalysts with compositional heterogeneity. Combined configuration facilitates the formation of Ce^{3+} and lattice defects, resulting in improved oxygen mobility, due to strong interaction between the noble metal and the support as well as the synergistic function inside the support. Consequently, the corresponding catalysts show amplified operation windows for the conversions of CO, C_3H_8 and NO before and after aging, indicating promising application in purification of automobile exhaust gases.

Key words: combined composition; sequential precipitation; Pd-only three-way catalyst; catalytic performance

Exhaust gas (mainly HC, CO and NO_x) from the internal combustion of automobile engines, which is a main cause of air pollution, has attracted much attention since the past decades. Up to now, many methods have been developed to deal with the above-mentioned harmful emissions, among which the three-way catalyst (TWC) is considered most effective[1]. CeO_2-ZrO_2-based oxide (CZ), owing to its redox property involving the Ce^{4+}/Ce^{3+} couple, is of great technological importance in TWC[1-2].

As is well known, the structure of CZ-based oxides plays an important role in determining the redox properties. Previous studies have disclosed that the atomically homogenous CeO_2-ZrO_2 solid solution exhibits excellent OSC[3-4]. However, a recent work has reported that the nanoscale compositional heterogeneity consisting of Ce-rich cores surrounded by Zr-rich shells gives rise to the creation of differential strain fields especially in the interfacial regions, resulting in intriguing low temperature reducibility[5]. Conversely, other groups have claimed that small Ce-rich particles on the surface of CZ could benefit the low temperature reducibility[6-7]. Moreover, another $Ce_{0.5}Zr_{0.5}O_2$ consisting of Ce-rich and Zr-rich domains with large interfacial area, was found to exhibit improved OSC[8].

Thus, it can be concluded that the combination of Ce-rich and Zr-rich components can modify the redox properties of CZ composites. However, to the best of our knowledge, there are no open literatures focusing on the effect of combination styles of Ce-rich and Zr-rich components on the properties of Pd/CZ catalyst. In this work, two Pd/CZ catalysts with combined components ($Ce_{0.35}Zr_{0.65}O_2$/$Ce_{0.65}Zr_{0.35}O_2$) were prepared by a simple sequential precipitation route. The physicochemical properties were investigated by a range of techniques to disclose the effect of the combination styles on the catalytic behaviors.

1 Experimental

1.1 Preparation of supports

Conventional $Ce_{0.35}Zr_{0.65}O_2$ and $Ce_{0.65}Zr_{0.35}O_2$ were prepared by co-precipitation route. An aqueous solution containing $Ce(NO_3)_3$ (Dongfeng Chemical Plant, Leshan, Sichuan, Chemically pure) and $ZrO(NO_3)_2$ (Jiangsu Yixing Xinxing Zirconium Industry Co., Ltd., Chemically pure) was coprecipitated with an ammonia solution (Chengdu

Received date: 2017-08-09; **Modified date:** 2017-11-08
Foundation item: National Hi-tech Research and Development Program of China (863 Program, 2015AA034603); Opening Project of Key Laboratory of Sichuan Institutes of Higher Education(15-S07, 16-R04)
Biography: LI Hong-Mei(1980–), female, PhD. E-mail: lihongmeihappy@126.com
Corresponding author: LAN Li, PhD. E-mail: wskadlb@163.com; CHEN Yao-Qiang, professor. Email: chenyaoqiang@scu.edu.cn

Kelong Chemical Reagent Factory, 25wt%) under vigorous stirring. During the process, the pH was controlled at about 10.0. The obtained precipitate was filtered, washed, dried at 120℃ and calcined at 600℃ for 3 h to get the fresh samples, which were assigned as Ce35-F and Ce65-F, respectively.

The other two materials with combined compositions, consisting of $Ce_{0.35}Zr_{0.65}O_2/Ce_{0.65}Zr_{0.35}O_2$ = 1 : 1 (wt%), were synthesized by a sequential precipitation route. In the first stage, the precursor of the inner component (*e.g.*, an aqueous solution of $Ce(NO_3)_3$ and $ZrO(NO_3)_2$ with Ce/Zr molar ratio of 0.35/0.65) was reacted with an ammonia solution (25wt%), and then the formed precipitate was attacked by the other aqueous solution (consisted of $Ce(NO_3)_3$ and $ZrO(NO_3)_2$ with Ce/Zr molar ratio of 0.65/0.35) and an ammonia solution (25wt%), contemporaneously. During the process the pH was maintained at 10.0. Afterwards the precipitate was treated as above to obtain Ce35i-F. In addition, Ce65i-F was prepared in the same way except for exchanging the precipitation sequence of the two aqueous solutions.

Finally, the above-obtained oxides were further aged at 1000℃ for 5 h and assigned as Ce35-A, Ce65-A, Ce35i-A and Ce65i-A, respectively.

1.2 Catalyst preparation

The Pd-only three-way catalysts were prepared by wet-impregnation method and Pd loading was 0.5wt%. The loading amount onto cylindrical cordierite monoliths (Corning, USA, 2.5 cm^3 and 400 cells·$in.^{-2}$) was 140 g/L. After being thermal treated at 550℃ for 3 h, the fresh catalysts designated as Pd/Ce65i-F, Pd/Ce35i-F, Pd/Ce65-F and Pd/Ce35-F were obtained. Finally, after being further treated at 1000℃ for 5 h, aged samples named as Pd/Ce65i-A, Pd/Ce35i-A, Pd/Ce65-A and Pd/Ce35-A were yielded.

1.3 Catalytic activity measurements

The three-way catalytic performance was estimated in a fixed-bed reactor with simulated exhaust gases of C_3H_8 (600 ppm), CO (0.86%), NO (800×10^{-6}), CO_2 (12%), H_2O (10%) and balanced with N_2. The gas hourly space velocity was 44000 h^{-1}. Prior to the test, the catalyst was pretreated under the reactive gas mixture at 550℃ for 1 h, and the air/fuel ratio test was carried out at 400℃. The conversions of C_3H_8, CO and NO were detected by an FGA-4100 analyzer.

1.4 Characterizations

XRD patterns were acquired on a Rigaku D/max-rA diffractometer using Cu Kα (λ = 0.15406 nm) as radiation and operated at 40 kV and 100 mA. Raman spectra were recorded on a LabRAM HR800 with 633 nm excitation wavelength.

The textural properties were determined by N_2 adsorption-desorption at 77 K on a Quantachrome automated surface area & pore size analyzer (Autosorb SI). The surface elemental composition was obtained using a British Kratos XSAM-800 electron spectrometer equipped with Mg Kα radiation (13 kV/20 mA).

Temperature programmed reduction (TPR) was analyzed using a self-assembled reaction system. The samples were firstly pretreated in flowing N_2 (25 mL/min) at 450℃ for 1 h. After cooling down to room temperature, the test was carried out under flowing 5% H_2/N_2 (20 mL/min) to 400℃ at a ramping rate of 8℃/min. Oxygen storage capacity (OSC) was examined by oxygen pulse injection technique. Prior to the measurement, the samples were reduced in H_2 (20 mL/min) at 550℃ for 1 h and then cooled to 200℃. Oxygen pulse was injected every 2 min to the samples in the stream of N_2 (25 mL/min) and the oxygen uptake was monitored by a TCD detector.

2 Results and discussion

2.1 XRD and Raman characterizations

Fig. 1 shows the XRD patterns of the catalysts. Note that the major peaks of all samples are typical of cubic fluorite CeO_2, indicating the formation of CeO_2-ZrO_2 solid solutions. From the inset in Fig. 1(a), it is seen that the 2θ value decreases in the sequence of Pd/Ce35-F > Pd/Ce65i-F ≈ Pd/Ce35i-F > Pd/Ce65-F, which is ascribed to the increasing Ce/Zr ratios of the samples. It is worthwhile to point out that no distinguishable separated phases can be observed, which is unexpected for Pd/Ce65i-F and Pd/Ce35i-F. According to the literatures[8-9], conventional diffraction analysis cannot distinguish the coexistence of micro-domains of Ce-rich and Zr-rich phases because the crystallographic structure and orientation of the atomic planes are the same. Therefore, it can be deduced that there exists strong interaction between the two components in Pd/Ce65i-F and Pd/Ce35i-F, making the Ce-rich and Zr-rich compositions indistinguishable.

After aging, all catalysts exhibit sharper peaks, indicating the presence of larger crystallites. As seen in Fig. 1(b), Pd/Ce65-A maintains single cubic phase, whereas for Pd/Ce35-A, a strong peak at 29.6° with a minor shoulder at 29.1° is displayed, indicating that the Ce-rich sample mainly undergoes sintering and severe phase segregation has happened for the Zr-rich sample. However, for Pd/Ce65i-A and Pd/Ce35i-A, no obvious phase separation is observed, the peaks are only somewhat asymmetric owing to the compositional heterogeneity. That is, the sintering of Ce-rich phase and segregation of Zr-rich phase are well suppressed, indicating their higher structural stability.

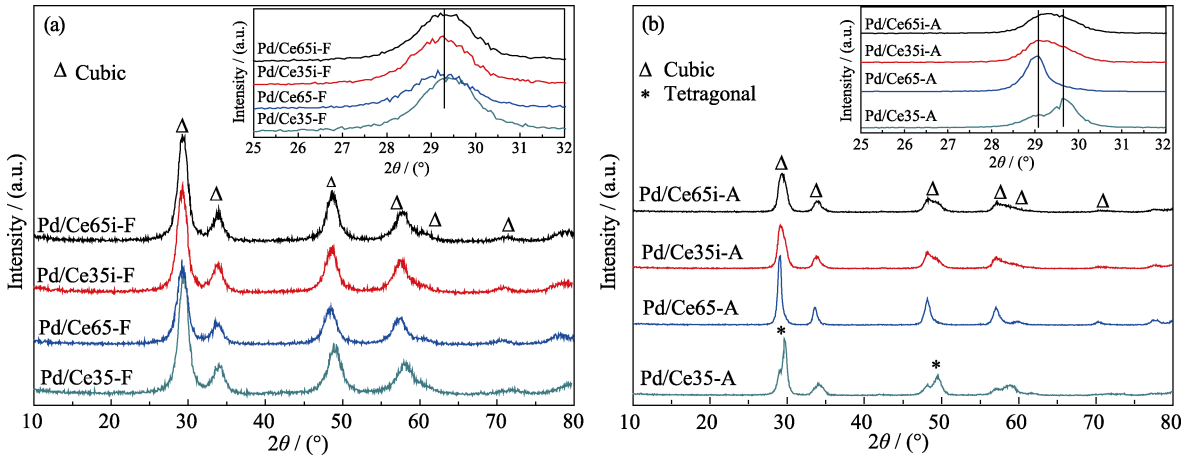

Fig. 1 XRD patterns of (a) fresh and (b) aged catalysts

Raman spectra of fresh and aged catalysts are shown in Fig. 2. For fresh samples, two main bands at ca. 472 cm^{-1} and 613 cm^{-1} are observed. The former is ascribed to the F_{2g} mode of cubic fluorite structure, and the later is due to the longitudinal optical (LO) mode of CeO_2 which is indicative of oxygen vacancies in the lattice[10]. It's observed that the intensities of the signals for the later peak are ordered as: Pd/Ce65i-F > Pd/Ce35i-F ≥ Pd/Ce65-F > Pd/Ce35-F, implying that the combined compositions, especially when $Ce_{0.65}Zr_{0.35}O_2$ is formed during the first step, can create more oxygen vacancies, which is beneficial for the redox properties.

After aging, peak sharpening occurs owing to the grain growth. However, it is not obvious for Pd/Ce35-A, in which two new bands centered at 246 cm^{-1} and 303 cm^{-1} are present, indicating the coexistence of cubic and tetragonal CZ phases[10], which is in line with the XRD results. However, weak peaks assigned to tetragonal phase are also found in Pd/Ce65i-A and Pd/Ce35i-A, which confirms the coexistence of two components in these two samples. In addition, it's worthwhile to point out that the oxygen vacancies, especially in Pd/Ce65i-A and Pd/Ce35i-A, still maintain at rather high levels, as evidenced by the relatively stronger features at 613 cm^{-1}.

2.2 Textural properties

Table 1 summarizes the textural parameters of the catalysts, wherein we can find that the composition of supports greatly affects the textural properties[11]. The surface areas of the fresh catalysts decrease in the order of Pd/Ce65-F > Pd/Ce65i-F > Pd/Ce35i-F > Pd/Ce35-F. Nevertheless, the pore volumes and average pore sizes of the catalysts with combined components are larger. After aging, the textural properties deteriorate severely for all samples, which results from the growth of primary particles and the phase separation, as evidenced by the XRD and Raman results. For the aged samples, the surface areas and pore volumes are ordered as Pd/Ce65i-A > Pd/Ce35i-A > Pd/Ce65-A > Pd/Ce35-A, suggesting that the combined composition can enhance the thermal stability.

Moreover, the pore size distributions (PSD) of fresh samples are presented in Fig. 3. The PSD of Pd/Ce65-F and Pd/Ce35-F show single peaks centered at 2.5 nm and 3.3 nm, respectively. Nevertheless, the PSD of Pd/Ce35i-F

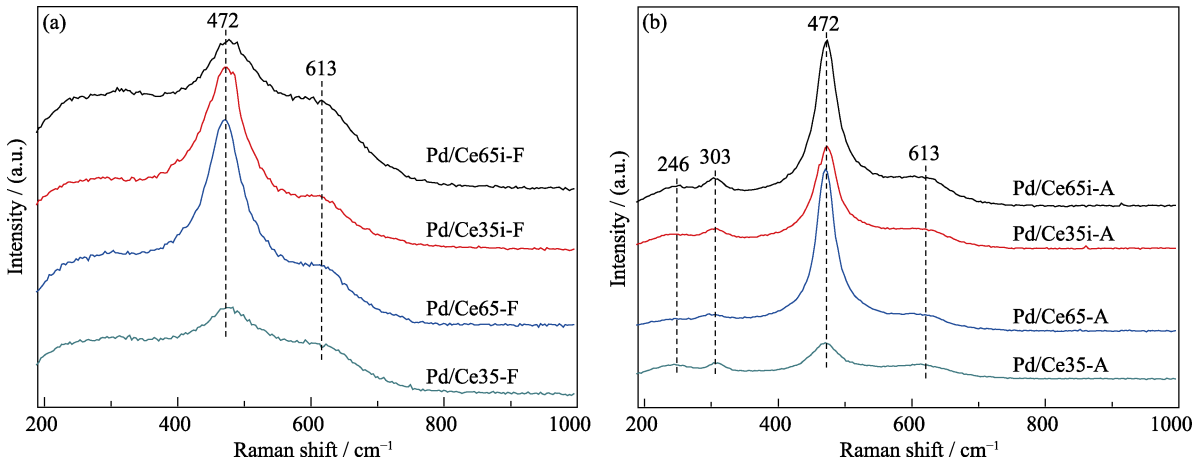

Fig. 2 Raman spectra of (a) fresh and (b) aged catalysts

Table 1　Textural properties of fresh and aged catalysts

Sample	Surface area /($m^2 \cdot g^{-1}$)		Pore volume /($ml \cdot g^{-1}$)		Average pore radius/nm	
	fresh	aged	fresh	aged	fresh	aged
Pd/Ce65i	125	26	0.29	0.15	4.6	11.2
Pd/Ce35i	122	25	0.26	0.14	4.3	11.0
Pd/Ce65	131	23	0.24	0.12	3.6	10.9
Pd/Ce35	117	17	0.25	0.11	4.0	13.9

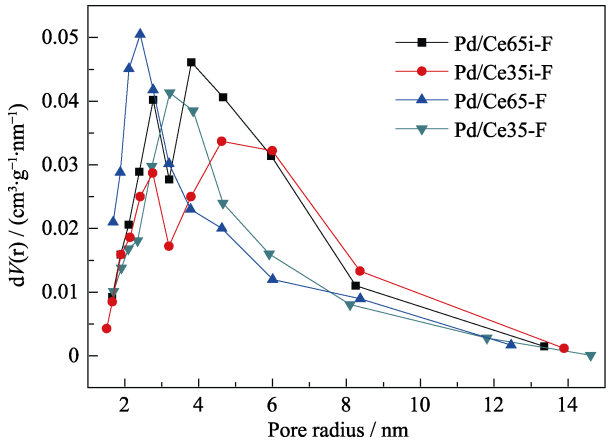

Fig. 3　Pore size distributions of the fresh catalysts.

and Pd/Ce65i-F show special bimodal features, which may be due to the coexistence of smaller and larger pores created by $Ce_{0.65}Zr_{0.35}O_2$ and $Ce_{0.35}Zr_{0.65}O_2$, respectively[11]. Thus the primary particles of $Ce_{0.65}Zr_{0.35}O_2$ and $Ce_{0.35}Zr_{0.65}O_2$ seem to stick together to form heterogeneous PSD, which is less sensitive to temperature[12]. Additionally, analogous to the "diffusion barrier" concept[13], the particles of $Ce_{0.65}Zr_{0.35}O_2$ and $Ce_{0.35}Zr_{0.65}O_2$ are expected to separate each other from conglomeration, which can help inhibit the growth of particles upon aging.

2.3　XPS studies

The surface elemental information derived from XPS analysis is presented in Table 2. It's observed that the Ce/Zr ratios of Pd/Ce65-F and Pd/Ce35-F are much lower than the theoretical values, indicating that Zr is concentrated on the surface. For Pd/Ce65i-F, the Ce/Zr ratio is close to that of $Ce_{0.35}Zr_{0.65}O_2$, while the value of Pd/Ce35i-F is extraordinarily lower than that of $Ce_{0.65}Zr_{0.35}O_2$, implying that precipitation of $Ce_{0.65}Zr_{0.35}O_2$ in the first step is more advantageous to obtain the so-called "core-shell" structure, which is likely due to that the Zr-rich component is intrinsically more favorable to locate at the surface[14]. After aging, the Ce/Zr ratio declines significantly for Pd/Ce35i-F and Pd/Ce65-F, suggesting the migration of Zr to the outer shell[14]. However, only slight variations are discovered for Pd/Ce65i-F and Pd/Ce35-F. On the other hand, the surface Pd contents become lower after aging, which is caused by sintering

Table 2　XPS results of fresh and aged catalysts

Samples	Atomic concentration/%				Ce/Zr	(Ce^{3+}/Ce) /%
	Ce3d	Zr3d	Pd3d	O1s		
Pd/Ce65i-F	7.5	13.7	1.2	77.6	0.5	21.2
Pd/Ce35i-F	8.5	13.9	1.2	76.4	0.6	19.0
Pd/Ce65-F	11.3	9.2	1.7	77.8	1.2	18.9
Pd/Ce35-F	5.8	16.3	1.4	76.5	0.4	18.7
Pd/Ce65i-A	7.0	13.4	1.2	78.4	0.5	20.7
Pd/Ce35i-A	6.9	13.9	1.1	78.1	0.5	18.9
Pd/Ce65-A	8.4	9.9	1.4	80.3	0.8	18.2
Pd/Ce35-A	6.0	15.8	0.8	77.4	0.4	17.7

of the support, dissociation of PdO and agglomeration to large Pd clusters. However, the surface Pd concentrations decrease to lesser extent for Pd/Ce35i-A and Pd/Ce65i-A, indicating that the combined composition can enhance the thermal stability of the noble metal dispersion, which is crucial to catalytic activity. Moreover, the fraction of Ce^{3+} is obtained by integration of Ce3d XPS peaks. The concentration of Ce^{3+} declines in the order of Pd/Ce65i > Pd/Ce35i > Pd/Ce65 > Pd/Ce35 both for the fresh and aged samples. Since the presence of Ce^{3+} is indicative of the generation of oxygen vacancies, it is deduced that the combined composition facilitates the formation of defective structure.

2.4　TPR and OSC measurements

H_2-TPR patterns of the catalysts are illustrated in Fig. 4. For fresh catalysts, the reduction mainly presents two features (α and β) in the low-temperature region (< 150℃), which are assigned to the reduction of highly dispersed PdO_x species and stable PdO_x species, respectively[15]. The reduction occurs at lower temperatures for Pd/Ce65i-F and Pd/Ce35i-F, indicating their stronger reduction ability. Meanwhile, two extra weak peaks (denoted as γ and δ) are well resolved for Pd/Ce65i-F and Pd/Ce35i-F, which are correlated with the reduction of bulk oxygen of CZ, implying the stronger interaction between Pd and CZ. After aging, only a couple of positive peaks (α′ and β′) are identified, which are considered to be the contribution of PdO and surface/subsurface oxygen. The lower intensity of α′ than α implies the agglomeration of PdO_x, which is induced by sintering and phase separation of the support. Pd/Ce65i-A and Pd/Ce35i-A exhibit better reducibility than Pd/Ce65-A and Pd/Ce35-A in terms of reduction temperature and peak area, which is associated with their enhanced interaction between noble metal and the support[4].

The oxygen storage capacity (OSC) values of the catalysts are shown in Fig. 5. It is found that the OSC values are closely associated with the composition of supports. For fresh catalysts, the OSC follows the order of Pd/Ce65i-F >

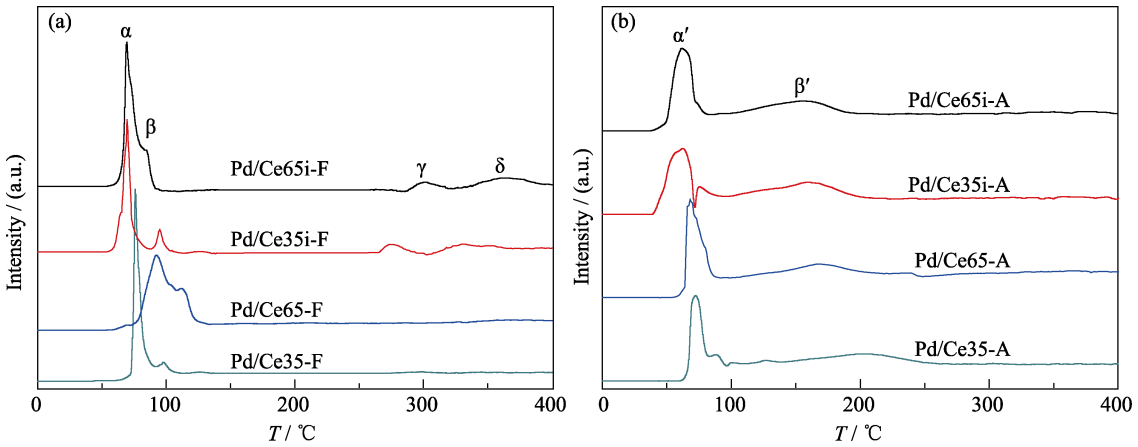

Fig. 4 TPR profiles of (a) fresh and (b) aged catalysts

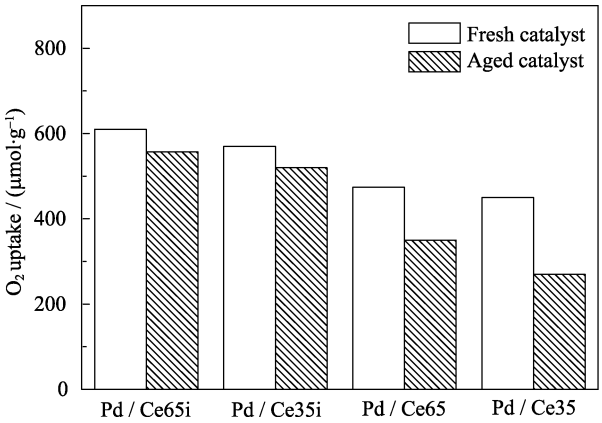

Fig. 5 OSC values of fresh and aged catalysts

Pd/Ce35i-F > Pd/Ce65-F > Pd/Ce35-F, after aging, the OSC values decrease collectively, while the values of Pd/Ce65i-A and Pd/Ce35i-A are still higher, implying that the combined compositions can significantly improve the oxygen mobility as well as its thermal stability.

2.5 Three-way catalytic performance

The catalytic performance results are presented in Fig. 6. For fresh catalysts, it is seen that Pd/Ce65i-F and Pd/Ce35i-F show better three-way catalytic activity. As claimed in the literatures[16-17], Pd species at more oxidative state are beneficial for the oxidation of CO/HC. Thus, the more oxidative state of Pd species owing to the strong interaction between Pd species and the supports in Pd/Ce65i-F and Pd/Ce35i-F is partly responsible for their excellent CO/HC performance. Furthermore, the reducibility of Pd species is crucial to the CO/HC oxidation activity[18]. Thus, the better reducibility of Pd/Ce65i-F and Pd/Ce35i-F is important for the participation of PdO/Pd and Ce^{4+}/Ce^{3+} during CO/HC oxidation. In addition, the oxygen vacancies associated with Ce^{3+} ions adjacent to the noble metal particles are considered as active sites for NO activation[19]. Thus, the higher Ce^{3+} concentrations of Pd/Ce65i-F and Pd/Ce35i-F from the XPS results may account for the improved NO reduction ability.

After aging, the catalytic activities for CO, C_3H_8 and NO decrease apparently, due to the sintering of both supports and noble metals. The catalytic performance shows the trend of: Pd/Ce65i-A > Pd/Ce35i-A > Pd/Ce65-A > Pd/Ce35-A. That is, the catalysts with combined compositions exhibit superior three-way catalytic performance compared with the conventional ones, especially for Pd/Ce65i-A.

2.6 Discussion about the combination modes

Considering the coexistence of Ce-rich and Zr-rich compositions in the samples derived from sequential precipitation route, the possible conformations are proposed and illustrated in Fig. 7. The Ce-rich and Zr-rich particles can intimately stick to each other at the nanoscale (a) or submicron scale (c, d). And the formation of Ce-rich and Zr-rich domains in an individual nanocrystalline (b) is also expected. Although the exact combination style is still uncertain, (c) and (d) models with layered structure are speculated to be more dominant, taking into account the usage of sequential precipitation route. Analogous to previous study[8], a large quantity of structural defects and enlarged interfacial area can be created at the interface of $Ce_{0.35}Zr_{0.65}O_2/Ce_{0.65}Zr_{0.35}O_2$, which is supposed to be the origin of mobile oxygen species. Additionally, Zr-rich phase is more prone to locate in the outer layer, thus Pd/Ce65i-F exhibits higher thermal stability than Pd/Ce35i-F. An inspiring conclusion can be drawn that the oxygen storage capacity is no longer restricted by the requirement to produce CeO_2-ZrO_2 materials with strict single-phase or high surface area.

3 Conclusions

In this study, a simple sequential precipitation route has been developed to synthesize Pd/CeO_2-ZrO_2 catalysts with combined compositions, which are compared with the conventional ones. In this way, the thermal stability of the catalysts is effectively enhanced. After calcination

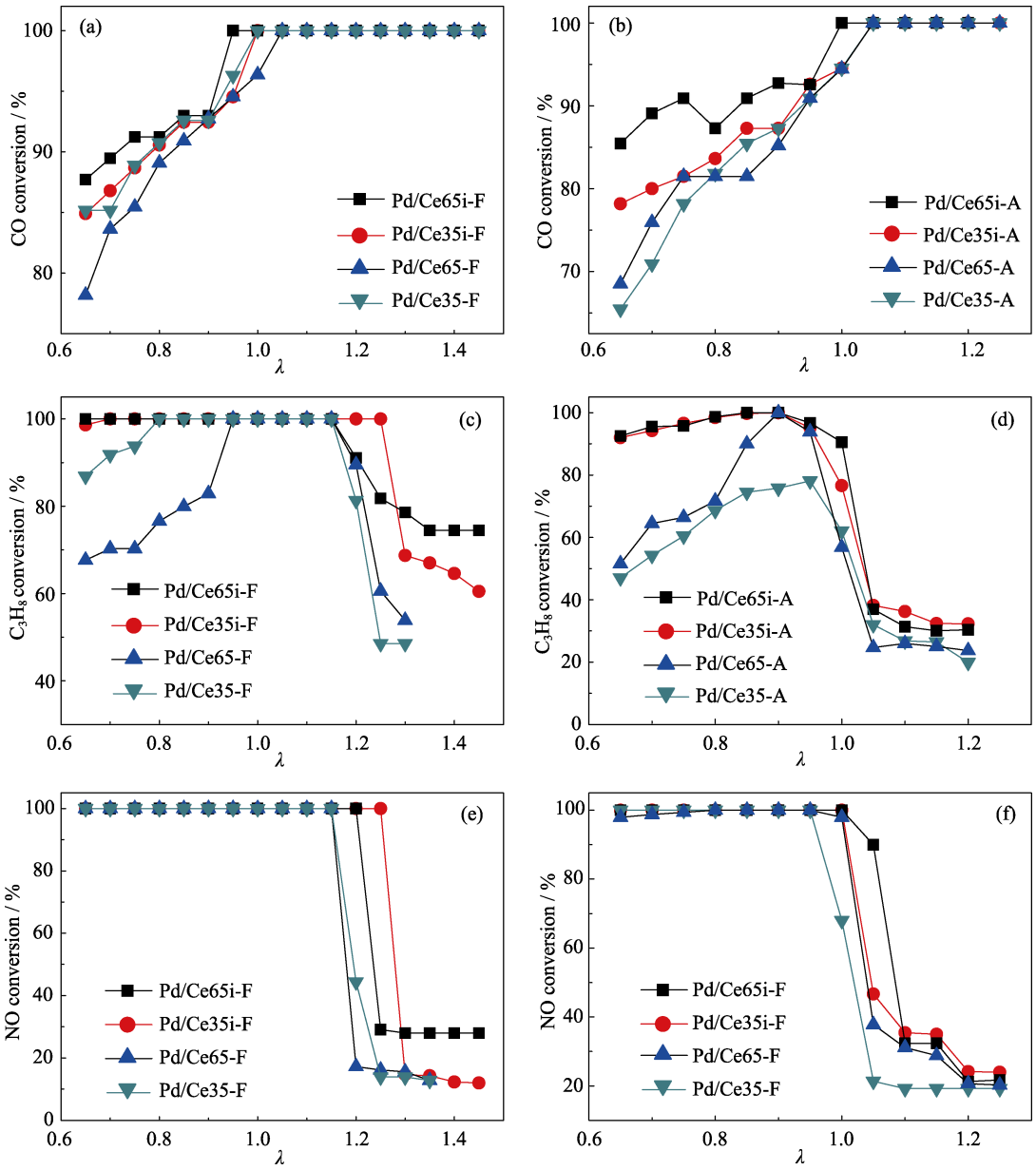

Fig. 6　Conversion curves of CO, C_3H_8 and NO as a function of air/fuel ratio (λ) of fresh and aged catalysts

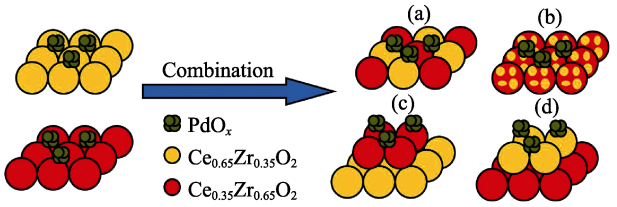

Fig. 7　Schematics of the combination modes of Pd/CeO_2-ZrO_2 catalysts prepared from sequential precipitation route

at 1000℃, different phase transformation and compositional reorganization behaviors can be observed. The special configuration facilitates the generation of Ce^{3+} and the improvement of redox properties, due to the strong interaction between noble metal and the support as well as the synergistic function between two components. The combination of the single components leads to advanced catalytic performance, in terms of enlarged three-way catalytic window, showing potential application in the purification of exhaust gases.

References

[1] KAŠPAR J, FORNASIERO P, GRAZIANI M. Use of CeO_2-based oxides in the three-way catalysis. *Catal. Today*, 1999, **50:** 285–298.

[2] WU Q F, CUI Y J, ZHANG H L, *et al.* Preparation of ceria-zirconia mixed oxides with improved thermal stability for three-way catalysts by a modified co-precipitation method. *J. Inorg. Mater.*, 2017, **32(3):** 331–336.

[3] NAGAI Y, YAMAMOTO T, TANAKA T, *et al.* X-ray absorption fine structure analysis of local structure of CeO_2-ZrO_2 mixed oxides with the same composition ratio (Ce/Zr = 1). *Catal. Today*, 2002, **74:** 225–234.

[4] ZHAO B, LI G, GE C, *et al.* Preparation of $Ce_{0.67}Zr_{0.33}O_2$ mixed oxides as supports of improved Pd-only three-way catalysts. *Appl.*

Catal. B: Environ., 2010, **96:** 338–349.

[5] WANG R G, CROZIER P A, SHARMA R, *et al.* Nanoscale heterogeneity in ceria zirconia with low-temperature redox properties. *J. Phys. Chem. B*, 2006, **110(37):** 18278–18285.

[6] MARTINEZ-ARIAS A, FERNANDEZ-GARCIA M, HUNGRIA A B, *et al.* Spectroscopic characterization of heterogeneity and redox effects in zirconium-cerium (1:1) mixed oxides prepared by microemulsion methods. *J. Phys. Chem. B*, 2003, **107(12):** 2667–2677.

[7] KOZLOV A I, KIM D H, YEZERETS A, *et al.* Effect of preparation method and redox treatment on the reducibility and structure of supported ceria-zirconia mixed oxide. *J. Catal.*, 2002, **209:** 417–426.

[8] MAMONTOV E, BREZNY R, KORANNE M, *et al.* Nanoscale heterogeneities and oxygen storage capacity of $Ce_{0.5}Zr_{0.5}O_2$. *J. Phys. Chem. B*, 2003, **107(47):** 13007–13014.

[9] SPECCHIA S, FINOCCHIO E, BUSCA G, *et al.* Surface chemistry and reactivity of ceria-zirconia-supported palladium oxide catalysts for natural gas combustion. *J. Catal.*, 2009, **263:** 134–145.

[10] SI R, ZHANG Y W, LI S J, *et al.* Urea-based hydrothermally derived homogeneous nanostructured $Ce_{1-x}Zr_xO_2$ (x=0–0.8) solid solutions: a strong correlation between oxygen storage capacity and lattice strain. *J. Phys. Chem. B*, 2004, **108:** 12481-12488.

[11] GONZALEZ-VELASCO J R, GUTIERREZ-ORTIZ M A, MARC J L, *et al.* Contribution of cerium/zirconium mixed oxides to the activity of a new generation of TWC. *Appl. Catal. B: Environ.*, 1999, **22:** 167–178.

[12] ROHART E, LARCHER O, DEUTSCH S, *et al.* From Zr-rich to Ce-rich: thermal stability of OSC materials on the whole range of composition. *Top. Catal.*, 2004, **30–31:** 417–423.

[13] MORIKAWA A, SUZUKI T, KANAZAWA T, *et al.* A new concept in high performance ceria-zirconia oxygen storage capacity material with Al_2O_3 as a diffusion barrier. *Appl. Catal. B: Environ.*, 2008, **78:** 210–221.

[14] BOZO C, GAILLARD F, GUILHAUME N. Characterisation of ceria-zirconia solid solutions after hydrothermal ageing. *Appl. Catal. A: Gen.*, 2001, **220:** 69–77.

[15] WANG Q, LI G, ZHAO B, *et al.* Synthesis of La modified ceria-zirconia solid solution by advanced supercritical ethanol drying technology and its application in Pd-only three-way catalyst. *Appl. Catal. B: Environ.*, 2010, **100:** 516–528.

[16] LI Z X, LI L L, YUAN Q, *et al.* Sustainable and facile route to nearly monodisperse spherical aggregates of CeO_2 nanocrystals with ionic liquids and their catalytic activities for CO oxidation. *J. Phys. Chem. C* 2008, **112:** 18405–18411.

[17] FERNDEZ-GARCIA M, IGLESIAS-JUEZ A, MARTINEZ-ARIAS A, *et al.* Role of the state of the metal component on the light-off performance of Pd-based three-way catalysts. *J. Catal.*, 2004, **221:** 594–600.

[18] LIU L, WEI T, ZI X, *et al.* Research on assembly of nano-Pd colloid and fabrication of supported Pd catalysts from the metal colloid. *Catal. Today*, 2010, **153:** 162–169.

[19] RAO G R, FORNASIERO P, MONTE R D, *et al.* Reduction of NO over partially reduced metal-loaded CeO_2-ZrO_2 solid solutions. *J. Catal.*, 1996, **162:** 1–9.

用于高性能单 Pd 三效催化剂的复合组分 $Ce_xZr_{1-x}O_2$ 材料的制备

李红梅[1], 兰 丽[1], 陈山虎[2], 刘达玉[1], 王 卫[1], 陈耀强[3]

(1. 成都大学 药学与生物工程学院, 成都 610106; 2. 中自环保科技股份有限公司, 成都 611731; 3. 四川大学 化学学院, 绿色化学与技术教育部重点实验室, 成都 610064)

摘 要: 用简单的顺序沉淀法制备了两种具有混合组分的 CeO_2-ZrO_2 材料。用 X 射线衍射(XRD), 拉曼光谱(Raman), X 射线光电子能谱(XPS), 氮气吸附–脱附, 氢气程序升温还原(H_2-TPR)和储氧量(OSC)研究了不同组合形式对负载的单 Pd 催化剂性能的影响。结果表明, 两个混和组分的催化剂结构和织构性能都得到了改善。由于贵金属和载体材料之间以及载体材料内部各组分之间的强相互作用, 组合的结构促进了Ce^{3+}和晶格缺陷的形成, 提高了氧的移动性, 并且相应的催化剂老化前后对于 CO、C_3H_8 和 NO 的转化都具有较宽的窗口范围, 说明这种具有混合组分的载体材料在汽油车尾气净化方面具有良好的应用前景。

关 键 词: 复合组分结构; 顺序沉淀法; 单 Pd 三效催化剂; 催化性能

中图分类号: TQ174 **文献标识码:** A